Journal of Nuclear Materials 395 (2009) 140–144

Contents lists available at ScienceDirect

Journal of Nuclear Materials

journal homepage: www.elsevier.com/locate/jnucmat

Diffusion behavior in an interface between U–10Zr alloy and HT-9 steel

Chong Tak Lee *, Hun Kim, Tae Kyu Kim, Chan Bock Lee

Korea Atomic Energy Research Institute, 1045 Daedeok-daero, Yuseong, Daejeon 305–353, Republic of Korea

ARTICLE INFO

Article history:
Received 5 December 2008
Accepted 7 October 2009

ABSTRACT

The diffusion behavior in an interface between a U–10 wt.%Zr alloy and HT-9 steel at 700 °C and 730 °C was investigated. The Zr-rich layer near the interface between two alloys was formed mainly due to the decomposition of the δ-UZr_2 phase in U–Zr alloy, and acted to interrupt the interdiffusion of the alloying elements. Considerable interdiffusion was observed only when the Zr-rich layer was destroyed locally. As a result, the diffusion–reaction layer was mainly composed of a U-rich, $(U,Zr)(Fe,Cr)_2$ compound, Zr-rich and Zr-depleted layers. Fe elements which had diffused from HT-9 were mainly observed in the boundaries of the Zr-rich particles in the U–Zr alloy.

1. Introduction

Metallic fuels such as U–Zr and U–PU–Zr alloys are being considered as nuclear fuels for sodium-cooled fast reactors (SFR) due to their excellent thermal conductivities, high densities and good breeding performance [1–5]. Ferritic/martensitic steels such as HT-9 and 9Cr steels are being recognized as candidate materials for the metallic fuel cladding tubes in SFRs due to their high thermal conductivities, low expansion coefficients and superior irradiation resistances to void swelling [6–10]. When the metallic fuels are applied to a nuclear fuel, their swelling results in an interdiffusion between the metallic fuels and cladding tubes. This interdiffusion induces the formation of intermetallic compounds that cause a degradation of the mechanical properties of the cladding tubes [11,12]. Hence, such interdiffusion behavior has become a subject of concern.

Some studies have reported that the interdiffusion behavior appeared to be dependent of the composition of the cladding materials, and HT-9 showed a thinner diffusion–reaction layer than Fe–18Cr–8Ni steel [13–15]. However, only limited results regarding U–Zr/HT-9 interdiffusion were reported. In addition, these papers report a diffusion behavior at 700 °C for less than 100 h, which is a relatively short term. Hence, this study focuses on the interdiffusion between U–10 wt.%Zr and HT-9 at 700 °C for 1000 h, as well as at 730 °C for 300 h.

2. Experimental procedure

A U–10 wt.%Zr alloy was prepared by a vacuum induction melting (VIM) process (Table 1). The alloy was homogenized at 900 °C for 100 h. HT-9 steel was also prepared by the VIM process (Table 2). The steel ingot was hot-forged at 1200 °C, followed by a normalizing at 1050 °C for 1 h and a tempering at 750 °C for 1 h. Air cooling was applied for all the heat treatments. The disk-type specimens with an 8 mm diameter and a 2 mm thickness were prepared by a machining of the U–10 wt.%Zr alloy and HT-9 steel, and their planes were polished by up to 0.05 μm-size alumina powders. The disk-type U–Zr specimen was arrayed between the disk-type HT-9 ones, and a set of these specimens was wrapped with a Ta foil to prevent a reaction with the apparatus made of type 316 stainless steel (Fig. 1). The specimens were compressively pressed with a torque of 70 Nm. The assembled diffusion couple was then sealed in a quartz tube, and an isothermal heat treatment was performed at 700 °C for 300, 500, 800 and 1000 h. An additional diffusion couple was heat-treated at 730 °C for 300 h.

After a heat treatment, the cross-sectional microstructure was observed by using a scanning electron microscope (SEM) with a back scattered electron mode for a compositional contrast, and elemental analyses were made by using an energy dispersive spectroscope (EDS) attached to a SEM. The crystalline structures were identified by using an X-ray diffraction (XRD).

3. Results and discussion

3.1. Diffusion behavior between U–10 wt.%Zr alloy and HT-9 steel

Fig. 2 shows the SEM images of an interface between the U–10 wt.%Zr alloy and HT-9 steel after a heat treatment at 700 °C for 300, 500, 800 and 1000 h. It was apparent that the diffusion–reaction layer formed in the interface between the two specimens increased with time, finally forming about a 10 μm thickness after 1000 h. After a heat treatment for 300 h, protruded U-rich phases and a Zr-rich layer were observed as an interface between the two specimens (Fig. 2a). As the diffusion proceeded, the U-rich

* Corresponding author. Tel.: +82 42 868 2375; fax: +82 42 868 8549.
E-mail address: ctlee@kaeri.re.kr (C.T. Lee).

0022-3115/$ - see front matter © 2009 Published by Elsevier B.V.
doi:10.1016/j.jnucmat.2009.10.044

Table 1
Chemical composition of U–Zr alloy (wt.%).

U	Zr	C	O	N
Bal.	10.2	0.0010	0.0151	0.0008

Table 2
Chemical composition of HT-9 steel (wt.%).

Fe	Cr	Ni	Mo	Mn	Si	C	W	V	Ti
Bal.	12.09	0.65	1.04	0.61	0.42	0.21	0.46	0.29	0.015

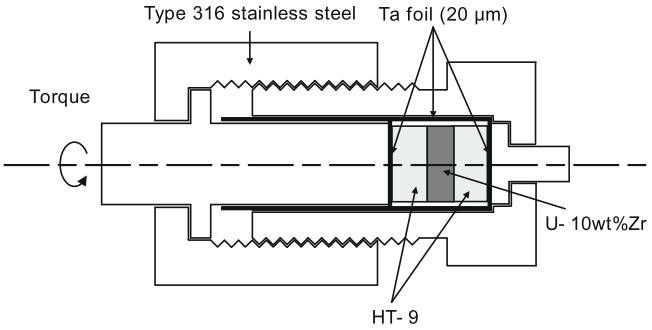

Fig. 1. Schematic drawing of the diffusion couple apparatus.

layers were extended along to the Zr-rich layer (Fig. 2b). As the diffusion proceeded further, they were further extended (Fig. 2c) and finally connected to each other after a heat treatment for about 1000 h (Fig. 2d). The SEM/EDS results of the reaction layer formed in an interface between the U–10 wt.%Zr and HT-9 after a heat treatment at 700 °C for 1000 h are shown in Fig. 3. The interdiffusion between the two specimens produced four distinctive diffusion–reaction layers from HT-9 to U–Zr alloys: U-rich, U–Fe compounds, Zr-rich, and Zr-depleted layers. The representative chemical composition of the U-rich phase was determined to be (at.%) 60U, 29Fe, 10Cr and 1Zr. In the U-rich layer marked as A in Fig. 3a, unreacted HT-9 particles were also observed. This observation means that the U atoms diffuse along to the grain boundaries of HT-9, and they spread parallel to the boundary between two alloys. Finally, they connect each other, forming the isolated HT-9 particles in the U-rich layer. Next was the U–Fe compound layer with about 6 μm in width marked as B, and its chemical composition was analyzed to be (at.%) 32U, 7Zr, 57Fe and 4Cr. Then, a Zr-rich layer with about 3 μm in width was observed marked as C, and its chemical composition was analyzed to be (at.%) 96Zr, 2U and 2Fe. The Zr-depleted layer marked as D was also observed in the U–Zr alloy, and its width appeared to be in the 5 μm range. The presence of Zr-rich and Zr-depleted layers indicates that the UZr_2 phases are decomposed into U and Zr elements, and the decomposed Zr elements are formed to the Zr-rich layer near an interface. It was reported that the Cr in the HT-9 might lead to an activation of the Zr in the UZr_2 to form a Zr-rich layer [15].

Fig. 4 shows the X-ray diffraction pattern obtained form the reaction layer between the U–10 wt.%Zr and HT-9 after a heat treatment at 700 °C for 1000 h. It was found that the reaction layer was mainly composed of several phases: U, Zr, U_6Fe, UFe_2, and Fe. It is believed that the U_6Fe, UFe_2 and Zr peaks are representative of the U-rich, U–Fe compounds and Zr-rich layers, respectively. Hence, the chemical formulations of the U-rich and U–Fe compound phases are believed to be U_6Fe and $(U,Zr)(Fe,Cr)_2$, respectively, which are in agreement with the previous studies [12–14].

Fig. 5 shows the SEM/EDS results from the reaction layer formed in an interface between the U–10 wt.%Zr and HT-9 after a heat

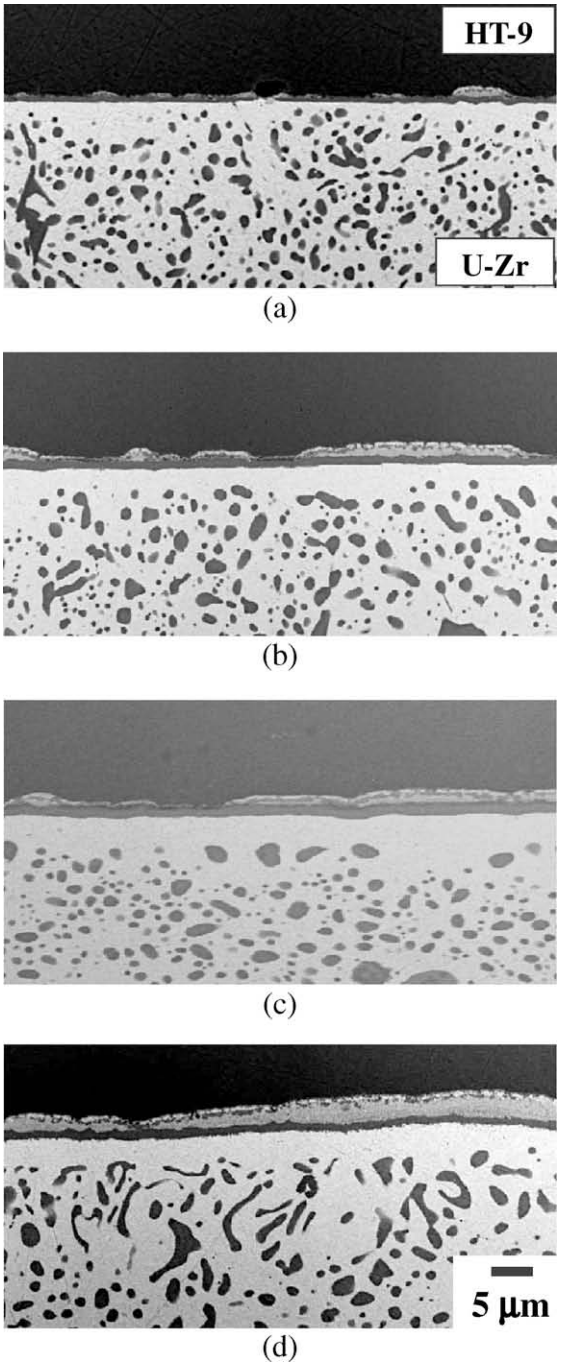

Fig. 2. SEM images on the interface between U–10 wt.%Zr alloy and HT-9 steel after a heat treatment at 700 °C for (a) 300, (b) 500, (c) 800 and (d) 1000 h.

treatment at 700 °C for 500 h. An examination of the distribution of the alloying elements showed that an Fe element was especially observed around the Zr-rich particles in the U–Zr alloy. This means that the Fe atoms which are diffused from the HT-9 to U–Zr alloy preferentially react with the Zr-rich particles more so than the U and δ-UZr_2 phases. It is thus considered that Fe has a higher affinity with Zr than U.

3.2. Correlation between diffusion–reaction and the Zr-rich layer

Fig. 6 shows the SEM images of the reaction layer formed in an interface between the U–Zr and HT-9 after a heat treatment at

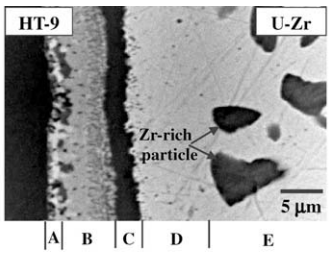

(a)

Layer marked in (a)	Phase	Representative composition (at.%)			
		U	Zr	Fe	Cr
A	U-rich phase	60	1	29	10
	Unreacted HT-9	2	-	84	14
B	$(U,Zr)(Fe,Cr)_2$	32	7	57	4
C	Zr-rich layer	2	96	2	-
D	Zr-depleted layer	96	3	1	-
E	α-U	96	4	-	-
	Zr-rich particle	2	97	1	-

(b)

Fig. 3. SEM image and EDS results in the interface between U–10 wt.%Zr and HT-9 after a heat treatment at 700 °C for 1000 h: (a) image and (b) representative chemical compositions from the layers marked in (a).

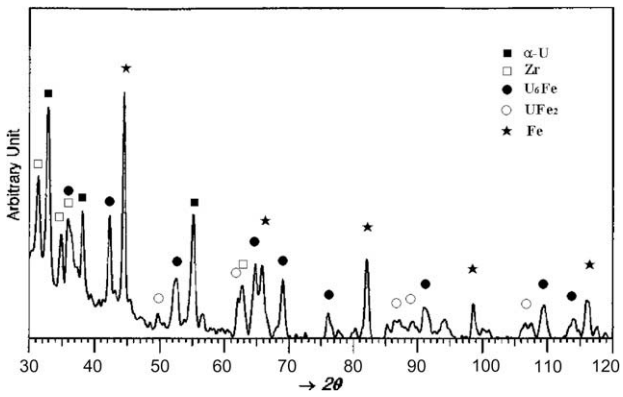

Fig. 4. X-ray diffraction pattern of the reaction layer between U–10 wt.%Zr and HT-9 after a heat treatment at 700 °C for 1000 h.

700 °C for 300 h. Two different diffusion behaviors were observed in the diffusion–reaction interface. A-type diffusion showed a higher thickness of the diffusion–reaction layers, such as U-rich and $(U,Zr)(Fe,Cr)_2$ compound layers, than the B-type one, while the B-type diffusion revealed a higher thickness of the Zr-rich layer than the A-type one. This means that there is a correlation between the Zr-rich and diffusion–reaction layers; a lower thickness of the Zr-rich layer always results in a higher thickness of the diffusion–reaction layer. The correlation for the thickness between the Zr-

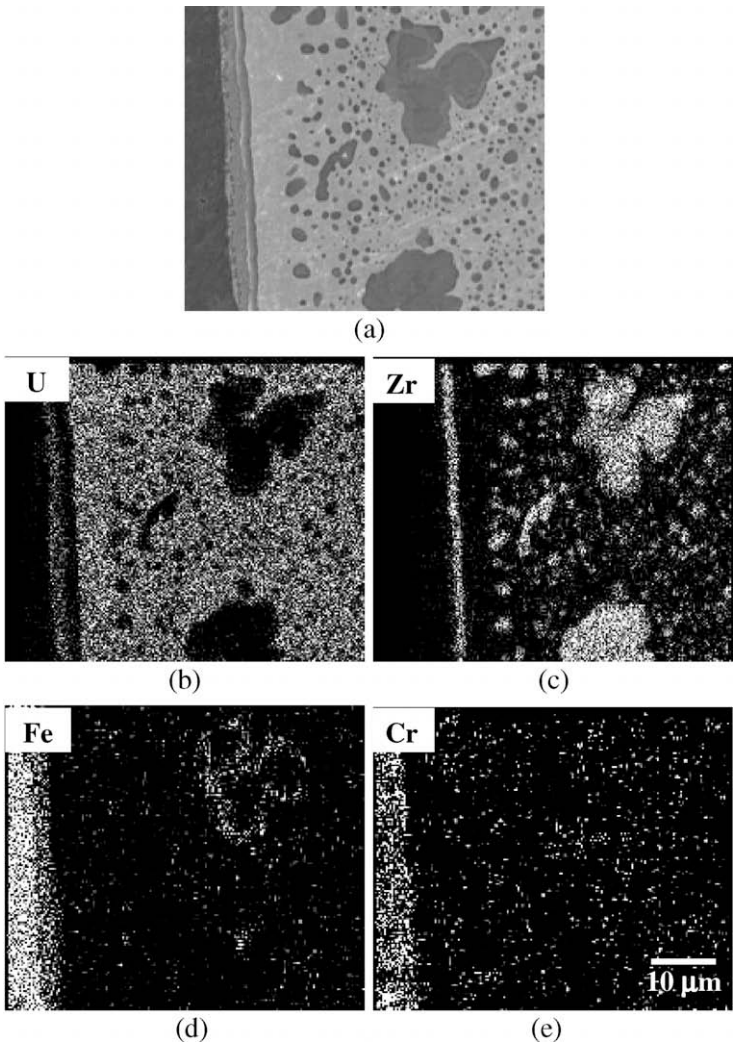

Fig. 5. SEM image and EDS results showing the distribution of alloying elements in the interface between U–10 wt.%Zr and HT-9 after a heat treatment at 700 °C for 500 h: (a) SEM image and mapping results of (b) U, (c) Zr, (d) Fe, and (e) Cr.

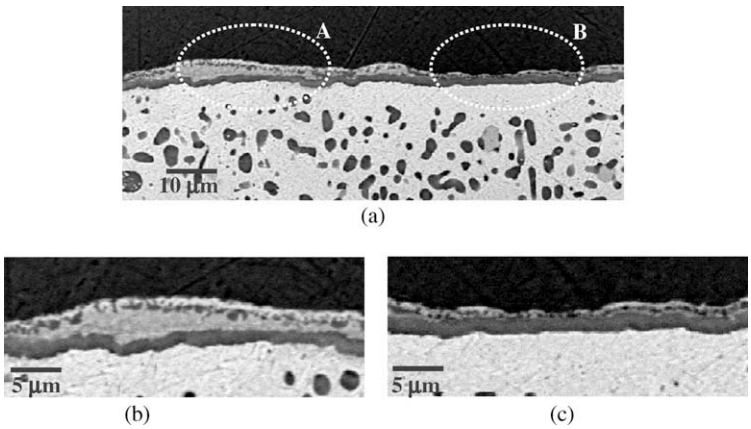

Fig. 6. SEM images showing two distinctive diffusion layer morphologies at interface formed after a heat treatment at 700 °C for 300 h: (a) two distinctive layers, (b) A-type layer marked by a dotted ellipsis in (a) and (c) B-type layer marked by a dotted ellipsis in (a).

rich and $(U,Zr)(Fe,Cr)_2$ layers is shown in Fig. 7. It was observed that the thickness of the U-rich layer in the A-type increased more rapidly than that in the B-type layer. These results demonstrate that the thicker Zr-rich layer acted to disturb the diffusion of the U atoms, resulting in a decrease in the formation rate of the diffusion–reaction layer.

3.3. Diffusion behavior

It is necessary to identify how the U elements diffuse through the Zr-rich layer, finally forming the UFe_2 phases between the HT-9 and Zr-rich layer. In addition, a slight increase in the temperature would be beneficial to observe the diffusion behavior, due to an increase in the diffusion rate. The microstructural observation for the interface between the U–10 wt.%Zr and HT-9 after a heat treatment at 730 °C for 300 h is shown in Fig. 8. A considerable amount of the U element with a dome-type shape was observed above the cracks of the Zr-rich layer. This observation indicates that a diffusion of U through a Zr-rich layer is possible when the Zr-rich layer has cracks. The reason for the cracks in the Zr-rich layer is not clear, but it is assumed that the driving force of the interdiffusion or the difference in the thermal expansion coefficient of the Zr-rich layer should cause the cracks in the Zr-rich layer.

Fig. 9 shows a schematic drawing illustrating the diffusion behavior between the U–10 wt.%Zr and HT-9 at 730 °C. Based on the SEM/EDS and XRD results (Figs. 2–8), the following prediction could be possible: in the first step, the δ-UZr_2 phases in the vicinity of the boundary layers between two specimens would decompose into U and Zr elements (Fig. 9a). The U elements in the U matrix would diffuse to the interface between the two specimens mainly forming a $(U,Zr)(Fe,Cr)_2$-type phase. At the same time, the Zr elements diffused from the decomposed UZr_2 phases should also be saturated to form a Zr-rich layer, acting as a barrier to an interdiffusion. This reaction results in the formation of a Zr-depleted (U-rich) layer between the Zr-rich layer and the U–Zr matrix (Fig. 9b). As the diffusion proceeds, cracks would occur in the Zr-rich layer, providing an easier path for an interdiffusion of the allowing elements as shown in Figs. 8 and 9c. As a result, the U elements would diffuse easily through the cracks in the Zr-rich layer into the HT-9. It is thus believed that the cracks in the Zr-rich layer

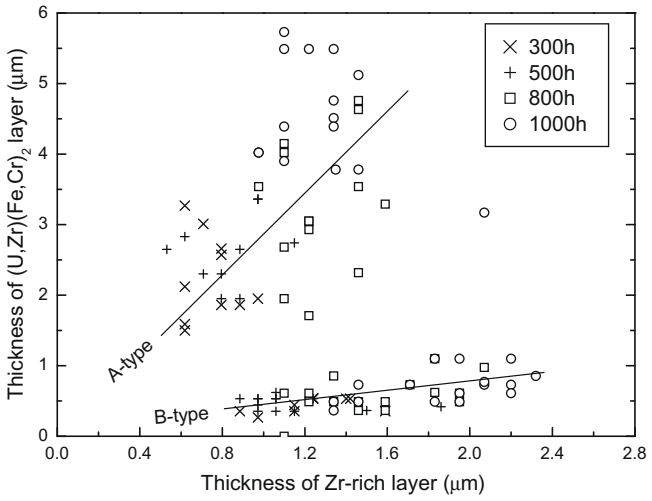

Fig. 7. Correlation between the thickness of Zr-rich layer and that of U-rich one, showing that the thickness of U-rich layer in A-type layer increases more rapidly than that in B-type layer.

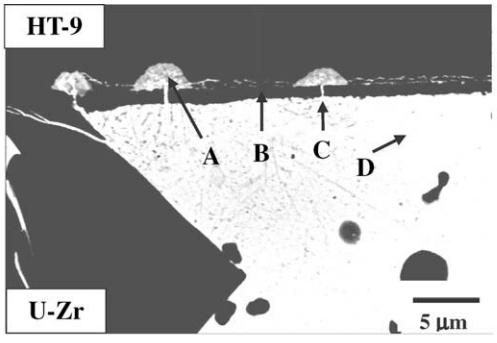

Position marked in (a)	Composition (at.%)			
	U	Zr	Fe	Cr
A	58	5	26	11
B	4	93	3	-
C	71	4	24	1
D	96	4	-	-

(b)

Fig. 8. SEM/EDS results after heat treatment at 730 °C for 300 h, indicating that the dome-type U elements from U–10 wt.%Zr alloy through cracks in Zr-rich layer: (a) SEM image and (b) EDS results marked by an arrow in (a).

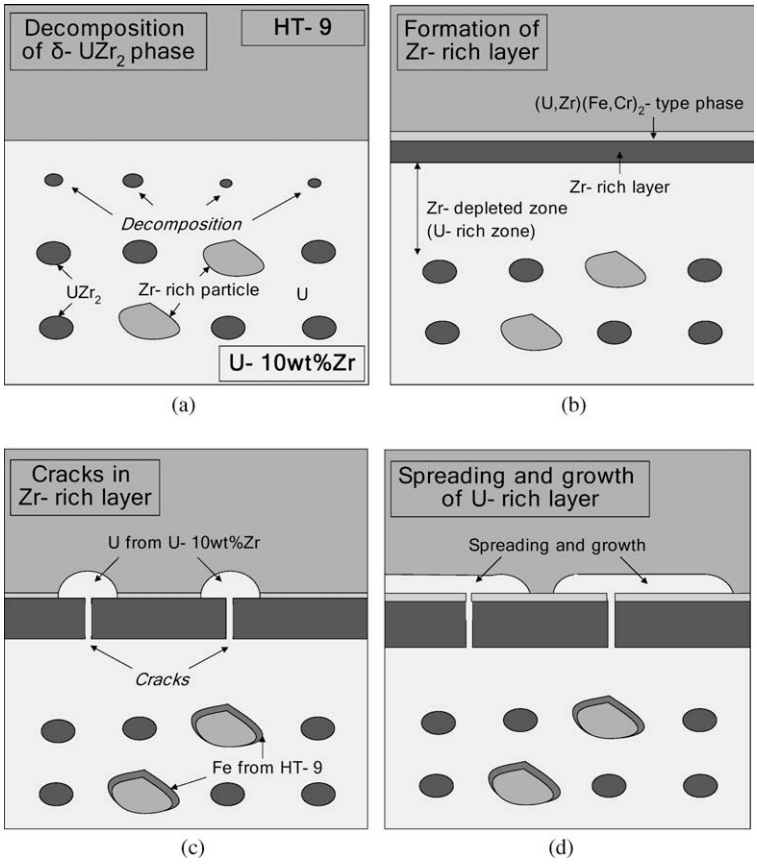

Fig. 9. Schematic drawing illustrating the interdiffusion behavior between U–10 wt.%Zr and HT-9 at 730 °C.

should provide the non-uniform thickness of the diffusion layer, as shown in Figs. 6 and 7. At the same time, the Fe elements diffused from the HT-9 through the cracks of the Zr-rich layer would reach the boundaries of the Zr-rich particles, forming an Fe–Zr compound, as shown in Figs. 5 and 9d.

4. Conclusions

The diffusion behavior in an interface between a U–10 wt.%Zr alloy and HT-9 steel was evaluated at 700 °C for up to 1000 h. After a diffusion reaction, the interface between the two specimens was mainly composed of four layers: U-rich, a U–Fe compound, a Zr-rich layer, and Zr-depleted ones. The unreacted HT-9 particles were observed in the U-rich layer. The Zr-rich layer was possibly formed due to a decomposition of the UZr_2 phase in the U–10 wt.%Zr alloy, resulting in the formation of the Zr-depleted (U-rich) layer. The Zr-rich layer acted to interrupt the interdiffusion of alloying elements. The U atoms from the U–Zr diffused into the HT-9, and they formed a localized U-rich zone only when the cracks in the Zr-rich layer were formed. It was also observed that the Fe atoms diffused through the interface and reached the boundaries of the Zr-rich particles, forming a new phase.

Acknowledgements

The authors would like to express their appreciation to the Ministry of Education, Science and Technology (MEST) of the Republic of Korea for their support of this work through the mid- and long-term nuclear R&D project.

References

[1] G.L. Hoffman, L.C. Walters, Mater. Sci. Technol. 10A (1994) 3.
[2] S.S. Hecker, M. Stan, J. Nucl. Mater. 383 (2008) 112.
[3] D.C. Crawford, D.L. Porter, S.L. Hayes, J. Nucl. Mater. 371 (2007) 202.
[4] C.E. Till, Y.I. Chang, W.H. Hannum, Prog. Nucl. Energy 31 (1997) 3.
[5] K. Nakamura, T. Ogata, M. Kurata, A. Itoh, M. Akabori, J. Nucl. Mater. 275 (1999) 246.
[6] F.A. Garner, M.B. Tgoloczko, B.H. Sencer, J. Nucl. Mater. 276 (2000) 123.
[7] R.L. Klueh, A.T. Lelson, J. Nucl. Mater. 371 (2007) 37.
[8] K.L. Murty, I. Charit, J. Nucl. Mater. 383 (2008) 189.
[9] T.K. Kim, J.H. Baek, C.H. Han, S.H. Kim, C.B. Lee, J. Nucl. Mater. 389 (2009) 359.
[10] T.K. Kim, S.H. Kim, C.B. Lee, Ann. Nucl. Energy 36 (2009) 1103.
[11] K. Nakamura, T. Ogata, M. Kurata, J. Phys. Chem. Solids 66 (2005) 643.
[12] D.D. Keiser Jr., M.A. Dayananda, Metall. Trans. A 25A (1994) 1649.
[13] T. Ogata, M. Kurata, K. Nakamura, A. Itoh, M. Akabori, J. Nucl. Mater. 250 (1997) 171.
[14] D.D. Keiser Jr., M.C. Petri, J. Nucl. Mater. 240 (1996) 51.
[15] D.D. Keiser Jr., M.A. Dayananda, J. Nucl. Mater. 200 (1993) 229.